[Short title + Author Name - P&H title] 17 (2024) 105983

Contents lists available at ScienceDirect

Arabian Journal of Chemistry

journal homepage: www.ksu.edu.sa

Original article

Highly efficient platinum nano-particles decorated multi-walled carbon nanotubes (Pt/MWCNTs) catalyst for catalytic hydrogenation of styrene–butadiene–styrene (SBS) copolymer

Alaaddin M.M. Saeed [a], Gui-Ping Cao [a,*], Ahmed S. Al-Fatesh [b], Salwa B. Alreshaidan [c], Nawab Ali [d], Mustapha Sani Shehu [a], Jun-Yang Yan [a]

[a] UNILAB, State Key Laboratory of Chemical Engineering, East China University of Science and Technology, Shanghai 200237, China
[b] Chemical Engineering Department, College of Engineering, King Saud University, P.O. Box 800, Riyadh 11421, Saudi Arabia
[c] Department of Chemistry, Faculty of Science, King Saud University, P.O. Box 800, Riyadh 11451, Saudi Arabia
[d] Shanghai Key Laboratory of Functional Materials Chemistry, School of Chemistry and Molecular Engineering, East China University of Science and Technology, Meilong Road 130, Shanghai 200237, China

ARTICLE INFO

Keywords:
Platinum
Multi-walled carbon nanotubes
Styrene-butadiene-styrene triblock copolymer
Cyclic block copolymer
Catalytic hydrogenation

ABSTRACT

This study presents the practical synthesis of platinum nanoparticle decorated multi-walled carbon nanotubes (Pt/MWCNTs) catalysts and their novel use in hydrogenating styrene–butadiene–styrene (SBS) triblock copolymers. The Pt/MWCNTs catalyst exhibited remarkable activity and selectivity in fully hydrogenating the polystyrene and polybutadiene segments within a styrene–butadiene–styrene (SBS) triblock copolymer. The characterizations proved that the Pt/MWCNTs catalyst possesses well-dispersed Pt nanoparticles with a large specific surface area (159.5501 m^2/g). Additionally, the catalyst is with a mesoporous structure. As a result, the catalytic hydrogenation of SBS using a Pt/MWCNTs catalyst achieves a high degree of hydrogenation, with 100 % selectivity towards the polystyrene and polybutadiene blocks in the SBS triblock copolymer at 180 °C after 9 h. The Pt/MWCNTs catalyst was characterized via SEM, TEM, HRTEM, XRD, XPS, Raman, TG, and BET. Simultaneously, the SBS and cyclic block copolymer (CBC) were characterized via GPC, FTIR, ^{1}H NMR, ^{13}C NMR, and TG. In this work, Pt/MWCNTs catalyst with high activity and selectivity is developed for unsaturated polymer hydrogenation.

1. Introduction

Selective hydrogenation of polymers containing benzene rings and unsaturated double bonds has been proven to be an effective process for improving the thermal, mechanical, and chemical properties of many polymers and copolymers (Khar'kova et al., 2011; Luo et al., 2019; Gu et al., 2021; Yan and Cao, 2023). Partially or fully hydrogenated polymers have versatile uses in high-end industries, including automotive components, smart textiles, medical devices, and protective coatings (Zhang et al., 2023). Catalytic hydrogenation is usually carried out using either homogeneous or heterogeneous catalysts (Chen et al., 2018; Wang et al., 2024; Yan et al., 2024).

The challenge of separating homogenous catalysts from the products renders their reuse problematic, resulting in a rise in the process cost (Miceli et al., 2021). Furthermore, the presence of the catalyst's heavy metal ions in the product leads to a decrease in the purity of the hydrogenated product and adversely affects the performance of the final product (Yang et al., 2012; Yang et al., 2013). Polymer products with low purity are significantly restricted in the food, medicinal, and other industries. As a result, certain scientists have anchored the active components (often metallic elements like Pd, Pt, Ru, Rh, etc.) onto unreactive carriers (such as $CaCO_3$, $BaSO_4$, SiO_2, CNTs, etc.) to create a three-phase hydrogenation reaction system involving gas, liquid, and solid phases, with H_2 and the reactant solution (Yan and Cao, 2023). After the reaction, the heterogeneous catalysts can be filtered out of the polymer solution, preventing metal contamination of the end products. In addition, heterogeneous catalysts can catalyse the hydrogenation process of unsaturated structures, such as benzene rings and C═C double bonds. (Yan and Cao, 2023). Heterogeneous catalysts are extensively utilized in polymer hydrogenation due to their superior resistance to elevated

* Corresponding author.
E-mail address: gpcao@ecust.edu.cn (G.-P. Cao).

https://doi.org/10.1016/j.arabjc.2024.105983
Received 28 May 2024; Accepted 28 August 2024
Available online 5 September 2024
1878-5352/© 2024 The Author(s). Published by Elsevier B.V. on behalf of King Saud University. This is an open access article under the CC BY-NC-ND license (http://creativecommons.org/licenses/by-nc-nd/4.0/).

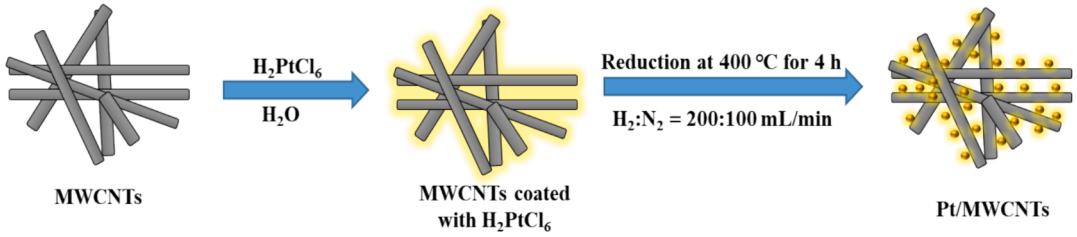

Fig. 1. Synthetic approach of Pt-MWCNTs.

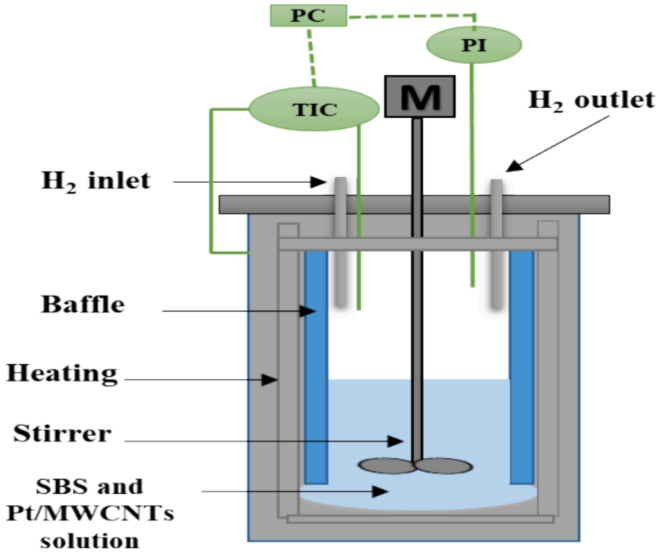

Fig. 2. Schematic illustration of the batch reactor for SBS hydrogenation reaction.

temperatures and pressures compared to homogeneous catalysts (Zhuchkov et al., 2021; Zou et al., 2023). Catalytic heterogeneous reactions are characterised by both internal and exterior diffusion, unlike homogeneous processes. The internal and exterior diffusion processes significantly influence heterogeneous reactions, particularly the reaction rate of polymer hydrogenation (Chen et al., 2018; Yan and Cao, 2023). The performance of heterogeneous catalysts is highly influenced by the surface area, pore structure, and carrier material (Pei et al., 2022; Zhang et al., 2022; Zhu et al., 2022a,b, Pei et al., 2023). The greater specific surface area enhances the even distribution of active components while enlarging the pore size can facilitate the entry of polymer macromolecules into the interior pores of the catalyst (Han et al., 2013).

In addition, multiple micro and/or mesoporous heterogeneous catalysts with a large specific surface area aid in better active metal dispersion. However, most of the active metal particles accumulate on the surfaces of the interior pores, making it challenging for polymer coils to reach the active sites. Conversely, non-porous catalysts like $CaCO_3$ and $BaSO_4$ have active sites on their outer surface and can prevent diffusion into pores. However, their surface area is restricted, and active metal distribution on the carrier is poor (Han et al., 2013).

It is known that carbon nanotubes (CNTs) are cylindrical carbon materials with a one-dimensional structure, characterized by their nanoscale diameter. Their aspect ratio is surprisingly high, with minimal micro-porosity and a substantial exterior surface area. In catalytic hydrogenation, CNTs have been used in many applications like selective hydrogenation (Guo et al., 2010; Chuang et al., 2012; Hemraj-Benny et al., 2018) and electro-oxidation reactions (Pang et al., 2010; Milone et al., 2011). Based on all the above-mentioned features, CNTs have been selected as carriers for our study.

Using platinum nanoparticles (Pt NPs) on MWCNTs for SBS catalytic hydrogenation has never been reported in the literature. Herein, Pt/MWCNTs catalyst was prepared using the chemical reduction method and applied to SBS heterogeneous catalytic hydrogenation for the first time. Based on the conducted experiments, the Pt/MWCNTs catalyst exhibited a high catalytic activity for polybutadiene and polystyrene blocks in a styrene–butadiene–styrene (SBS) with cyclohexane as solvent.

2. Experimental section

2.1. Materials

Multi-walled carbon nanotubes (Industrial grade with above 95 % purity) with 8–15 nm diameter and 30–50 μm length were purchased from Chengdu Organic Chemicals Co Ltd. H_2 (>99.9 %) was purchased from Shanghai Siling Gas Co., Ltd. SBS with a molecular weight of 169,927 g/mol. Cyclohexane was purchased from Shanghai Aladdin Biochemical Technology Co., Ltd. Chloroplatinic acid hydrate (>99.9 % Pt = 38 %) was purchased from Shanghai Jiuling Chemical Co., Ltd. Sodium Thiosulfate (99 %), Potassium iodide (99 %), and Iodine monochloride (98 %) were supplied by Acros Organics Co., Ltd.

2.2. Preparation of catalyst

The wetness impregnation method (Han et al., 2013; Gonçalves et al., 2022) was followed for the preparation of Pt/MWCNTs catalyst. The standard protocol for preparing Pt/MWNCNTs involved the following steps: 4 g of MWCNTs were immersed in 70 g of deionized water and dispersed for 15 min in an ultrasonic bath. An appropriate amount of chloroplatinic acid hydrate ($H_2PtCl_6{\cdot}6H_2O$) was dissolved in 10 g of deionized water and added dropwise to the suspension, dispersed for 60 min in an ultrasonic bath, and then stirred vigorously for 2 h at room temperature. The $H_2PtCl_6{\cdot}6H_2O$/MWCNTs suspension was filtered and dried at 80 °C for 10 h. Finally, the mixture was reduced under a stream of N_2 (100 mL/min) and H_2 (200 mL/min) for 4 h at 400 °C. The steps for MWCNTs decoration are summarized in Fig. 1.

2.3. Catalytic hydrogenation of SBS

The SBS catalytic hydrogenation reaction was conducted in 250 mL stainless steel high-pressure agitated autoclave (Fig. 2). A typical procedure is as follows. 100 g SBS dissolved in cyclohexane (3 wt%) solution was charged into the reactor. The powdered catalyst (Pt/MWCNTs) was directly dispersed into the reactant solution to form a slurry phase. The reactor was sealed and flushed with H_2 three times to remove air. After that, the reactor was heated to a desired temperature and then flushed with H_2 to a certain amount. After nine hours of the reaction, the solution was filtered out to separate the catalyst and the final hydrogenated product.

The hydrogenation degree of double bonds C═C (HD_{PB}) was analysed by bromo-iodometry method (Luo et al., 2019; Cao et al., 2024). The below formula is used to calculate the hydrogenation degree (HD_{PB}):

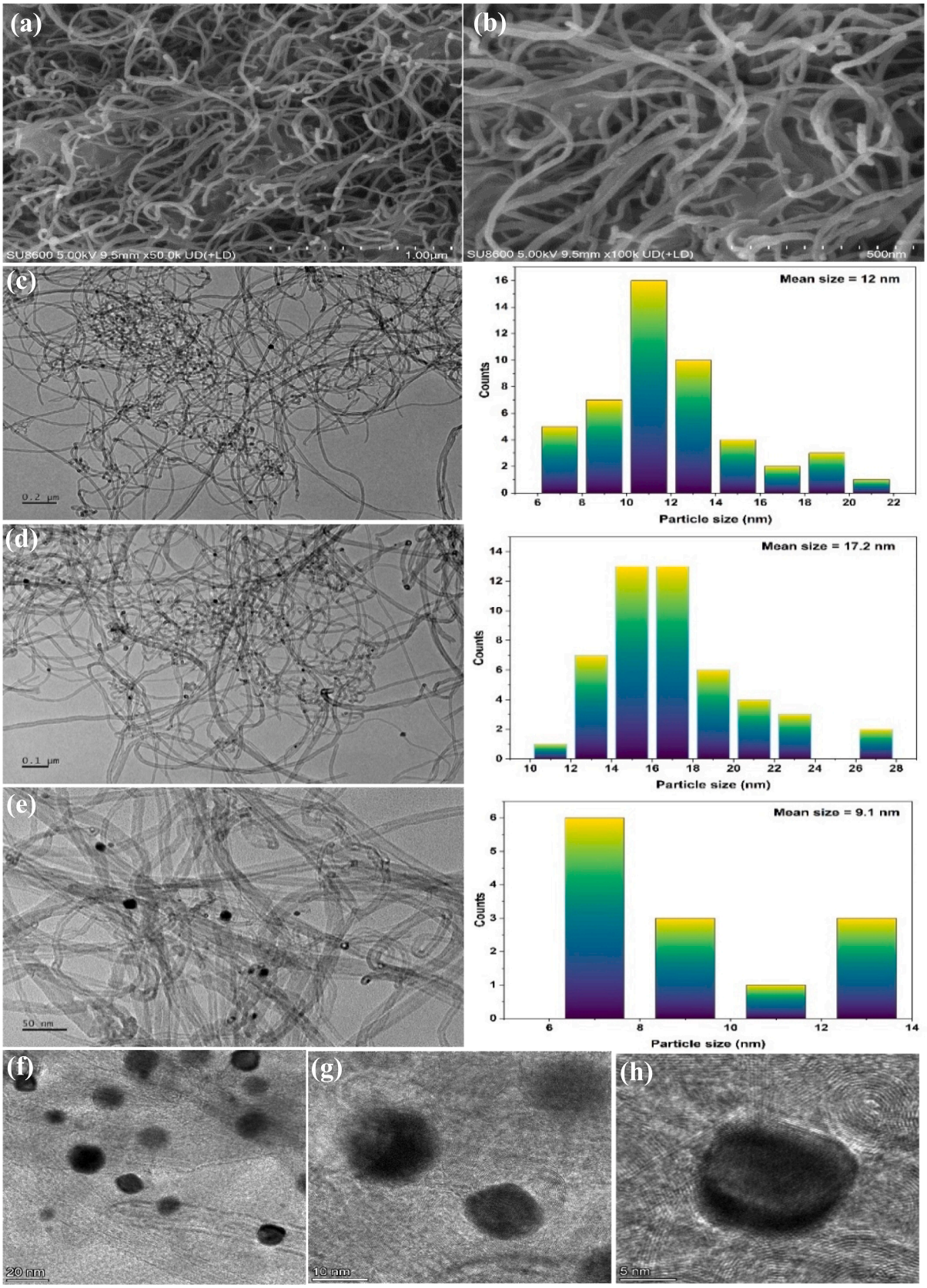

Fig. 3. SEM images of Pt/MWCNTs at (a) 1000 nm, and (b) 500 nm; TEM images of Pt/MWCNTs at (c) 200 nm, (d) 100 nm, and (e) 50 nm; HRTEM of Pt/MWCNTs at (f) 20 nm, (g) 10 nm, and (h) 5 nm.

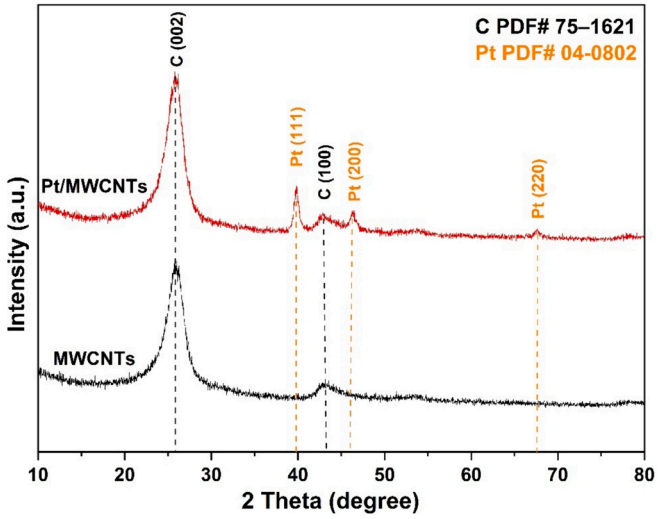

Fig. 4. XRD patterns of MWCNTs carrier and Pt/MWCNTs catalyst.

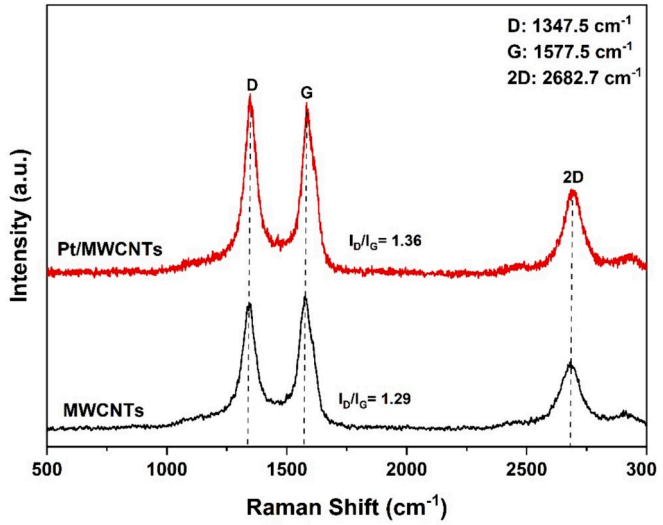

Fig. 5. Raman spectra of MWCNTs and Pt/MWCNTs composites.

$$HD_{PB} = \frac{C_{B0} - C_B}{C_{B0}} \times 100\% \quad (1)$$

where C_{B0} (mol/L) is the concentration of C═C before hydrogenation and C_B (mol/L) is the concentration of C═C after hydrogenation.

The hydrogenation degree of the benzene ring (HD_{PS}) was analysed by a UV–visible spectrophotometer (Cao et al., 2024; Yan et al., 2024) The benzene ring has a characteristic absorption peak at the wavelength of 261.5 nm, while the cyclohexane group and solvent cyclohexane have no absorption at this wavelength. The below formula is used to calculate the hydrogenation degree (HD_{PS}):

$$HD_{PS} = 1 - \frac{A}{A_0} \times 100\% \quad (2)$$

where A (mol/L) represent the concentration of benzene ring before hydrogenation and A_0 represent the concentration of the benzene ring after hydrogenation. The rest of the polymer solution was dried in the vacuum oven at 40 °C and −0.1 MPa to a constant weight.

2.4. Characterizations

Scanning electron microscopy (SEM) was conducted via Regulus8100 (Hitachi). Transmission electron microscopy (TEM) was done by jeol-jem2100F (JEOL). High Resolution transmission electron microscopy (HRTEM) was done by FEI Talos F200x (United States). X-ray diffraction (XRD) analyses were recorded on an X'Pert3 Powder (PANalytical B.V.) X-ray photoelectron spectroscopy (XPS) measurements were carried out via ESCALAB 250Xi. N_2 Physisorption (BET) was performed via ASAP2020 (Micromeritics). Nuclear magnetic resonance (NMR) spectroscopic samples analysis was employed on Bruker Avance 400 (BRUKER), using $CDCl_3$ as the solvent. Fourier transform infrared (FTIR) spectra were conducted via Nicolet (Thermo Fisher). Gel Permeation Chromatography (GPC) was conducted via waters1525 (Waters). Differential thermal analysis (DTA) was determined via Mettler (Swiss TGA2).

3. Results and discussion

3.1. Structure and morphology of catalyst

Typical scanning electron microscopy (SEM) and high resolution transmission electron microscopy (HRTEM) images of the Pt/MWCNT catalyst are shown in Fig. 3. The dark spots on the walls of the carbon nanotubes correspond to Pt nanoparticles (Kardimi et al., 2012). The MWCNT carriers have a tubular structure. The Pt NPs on MWCNTs are uniformly dispersed on MWCNTs with a mean particle size that is 9–17 nm according to TEM statistical calculations.

Fig. 4 displays the X-ray diffraction (XRD) pattern of the MWCNT carrier and the Pt/MWCNTs catalyst. The obtained diffraction peaks were compared to the standard International Centre for Diffraction Data (ICDD) for graphite and platinum (graphite: 75–1621 and platinum: 04–0802). The MWCNTs have characteristic peaks of graphitic carbon at 25.9 and 43.4 which correspond to the (0 0 2) and (1 0 0) planes (Yao et al., 2019), respectively. The three peaks corresponding to the (1 1 1), (2 0 0), and (2 2 0) crystallographic planes of the face-centered cubic (fcc) structure of platinum were identified (Bonet et al., 1999; Tong et al., 2007; Krishnapriya et al., 2023). There were no detected peaks of oxidized Pt. This confirms the successful synthesis of a Pt NPs and MWCNTs composite material.

Fig. 5 shows the standard Raman spectrum of the MWCNTs carrier and Pt/MWCNTs catalyst. The three peaks observed at 1347.5 cm^{-1}, 1577.5 cm^{-1}, and 2682.7 cm^{-1} can be attributed to the D band (disordered carbon band), G band (graphite/ordered carbon band), and 2D band (indicating the second-order harmonic), respectively. (Li et al., 2016). In the Pt/MWCNTs, the intensity ratio of the D and G bands (ID/IG) is 1.36, which is greater than the ID/IG ratio of 1.29 in the MWCNTs. The higher ID/IG value over Pt/MWCNTs indicates the presence of more amount of defective carbon/disordered carbon than ordered carbon (Wei et al., 2022).

The textural properties of MWCNTs and Pt/MWCNTs were analyzed by N_2 physisorption, as shown in Fig. 6. The isotherm of Pt/MWCNTs complements the isotherm of Type IV, as classified by the International Union of Pure and Applied Chemistry (IUPAC). This isotherm is characteristic of the catalyst's mesoporous structure (Avcioglu et al., 2015; Jin et al., 2024). In addition, the hysteresis loops characterized by parallel and steep adsorption–desorption branches were classified as Type H1 per the IUPAC system. The specific surface area and pore volume of MWCNTs and Pt/MWCNTs are 178.6016 m^2/g, 0.663876 cm^3/g, 159.5501 m^2/g, and 0.667821 cm^3/g, respectively, as determined by the BET and BJH methods.

In addition, the chemical valence states of surface elements of Pt/MWCNTs had also been determined by XPS in Fig. 7. The high-resolution Pt 4f7/2 spectrum of Pt/MWCNTs was divided into two peaks at 71.6 and 72.7 eV, which are attributed to Pt (0) Pt (II) species, respectively (Ma et al., 2017). As illustrated in Fig. 7, the C 1s spectrum was decomposed into two characteristic peaks: C sp^2 at 284.8 eV and C sp^3 at 286. 1 eV, respectively (Jin et al., 2024).

The thermal stability of MWCNTs and Pt/MWCNTs was investigated

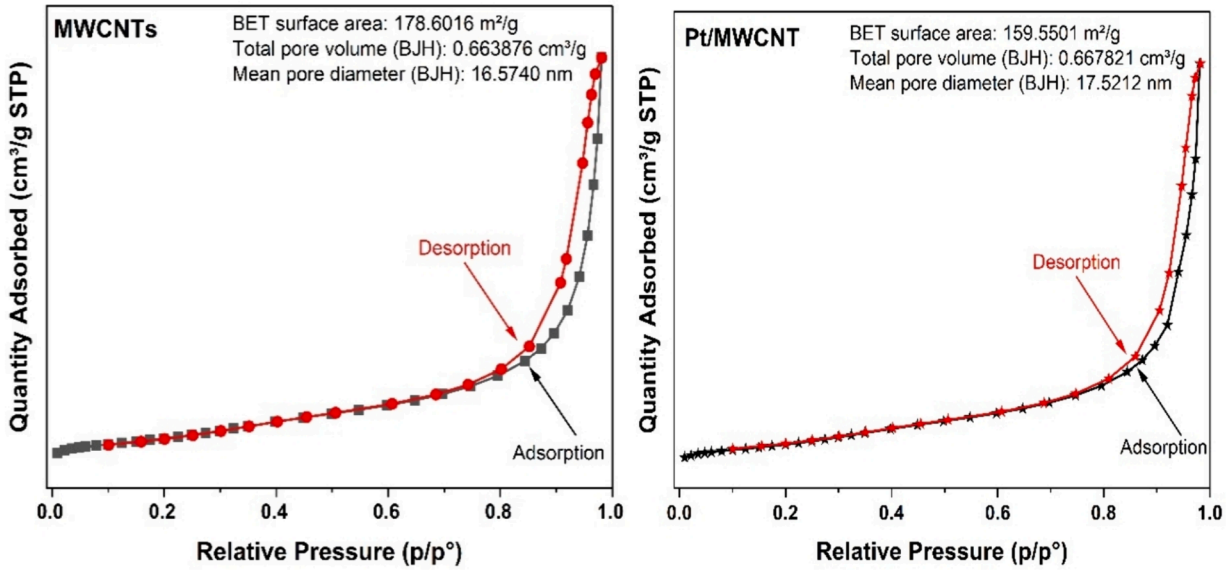

Fig. 6. Adsorption–desorption isotherms of MWCNTs and Pt/MWCNTs catalyst.

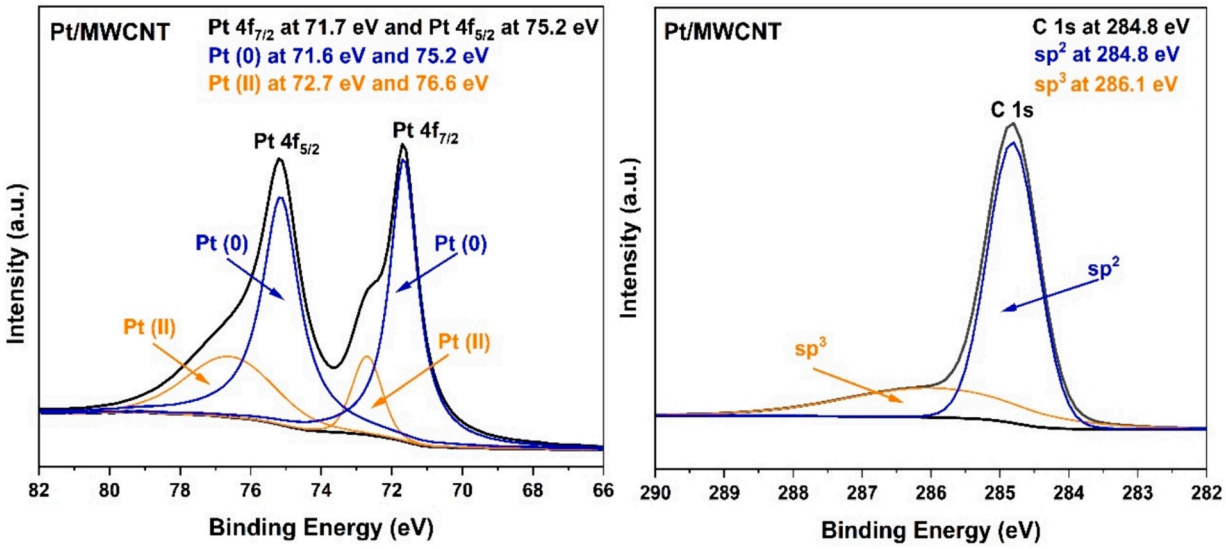

Fig. 7. High-resolution XPS spectra of C 1s and Pt/MWCNTs.

by thermal gravimetric analysis (TGA). Thermogravimetric curves of MWCNTs, and Pt/MWCNTs recorded in the temperature range of 100–800 °C at a constant heating rate of 10 °C per min under nitrogen atmosphere have been presented in Fig. 8. Thermogram shows that MWCNTs and Pt/MWCNTs are thermally stable. MWCNTs starts to decompose at 680 °C while Pt/MWCNTs starts to decompose at 667 °C. This indicates that the presence of platinum has slightly influence the thermal stability of the MWCNTs, potentially due to interactions at the nanoscale that alter the thermal degradation pathways. Overall, the Pt/MWCNTs exhibit a high thermal stability.

3.2. Hydrogenation mechanism of SBS over Pt/MWCNTs

In the process of heterogeneous catalytic hydrogenation of polymers, the molecules must be able to traverse the pores of the catalyst to access the active sites contained within. Furthermore, it is essential that the hydrogenated product possesses the capability to move out of the pores. Heterogeneous catalytic processes exhibit both internal and exterior diffusion. The heterogeneous catalytic hydrogenation of SBS is divided into six stages, as illustrated in Fig. 9.

Raman spectra validate the presence of more defective carbon over Pt/MWCNTs than MWCNTs. More defective carbon can trap “Pt”, enhances the interactions between the Pt and CNT, and improve the stability of the composite as a catalyst (Chen et al., 2013). Overall, stable Pt/MWCNTs is ready for catalyzing hydrogenation reaction. The reactants undergo adsorption on the catalyst’s active sites through both internal and exterior diffusion. The H_2 molecule dissociates on the surface of the metal or directly participates in the reaction according to the Horiuti-Polanyi mechanism (Yan and Cao, 2023). The reaction mechanisms of benzene rings and C═C double bonds are shown in Fig. 10. In the case of benzene rings: H_2 is activated on Pt and dissociated into 2 hydrogen atoms, and then forms an σ bond with platinum atoms to form the intermediate PtH. Paired electrons on the C−C π bond of the benzene ring also transfer and form a covalent σ bond with Pt, generating the intermediate Pt–C_6H_6. Finally, the two intermediates react, and the platinum atom on the benzene ring is replaced by a hydrogen atom. This process repeats continuously until the benzene ring is completely hydrogenated. In the case of C═C double bonds: At the beginning of the

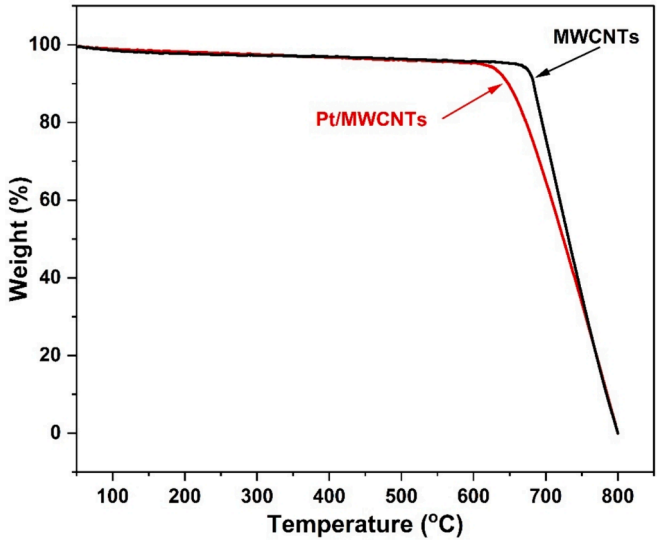

Fig. 8. TG thermograms of MWCNTs and Pt/MWCNTs.

reaction, H_2 is catalytically activated on the Pt surface and undergoes dissociation, forming two atoms of hydrogen. The atoms of hydrogen pass through the octahedral gap of the Pt lattice and form PtH with Pt. Simultaneously, the paired electrons on the π bond of C═C undergo transfer, forming σ bonds with two nearby Pt atoms on the crystal surface. The hydrogen atom replaces the platinum atom that is bonded to the carbon atom in PtH, and the resulting product is released following reduction.

In addition to the reaction mechanism of benzene rings and C═C double bonds on Pt, the carrier material and polymer interaction behavior are also important. Using spectroscopic and microscopic methods, J. N. Coleman (McCarthy et al., 2002) investigated the interaction between conjugated polymer and CNTs and found that the

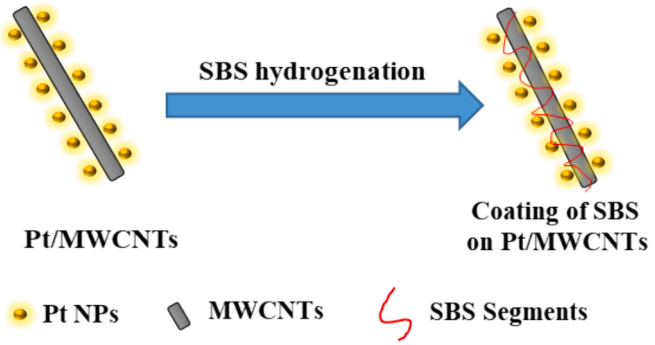

Fig. 11. Simulative view of Pt/MWCNTs catalyst and SBS segments interaction.

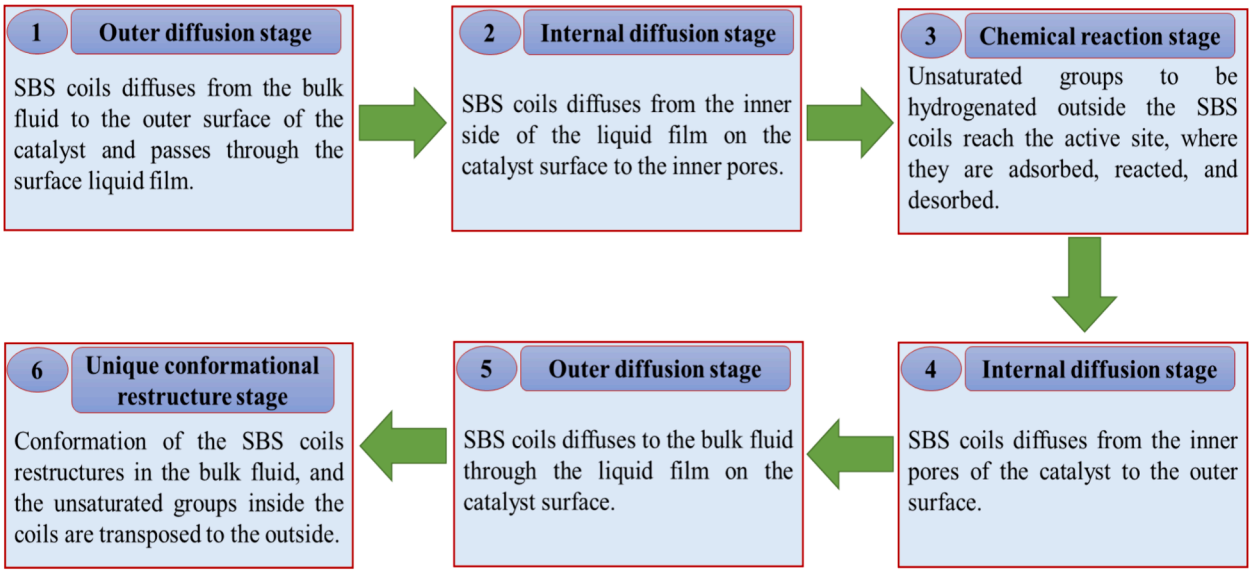

Fig. 9. SBS heterogeneous catalytic hydrogenation stages.

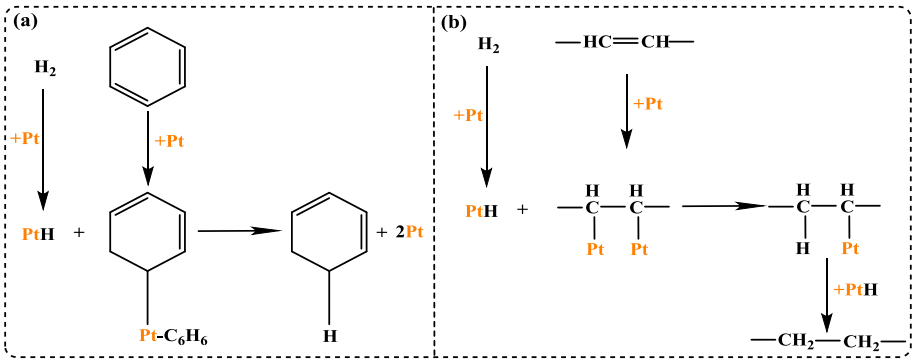

Fig. 10. Hydrogenation mechanism of (a) benzene rings, and (b) C═C double bonds on Pt NPs.

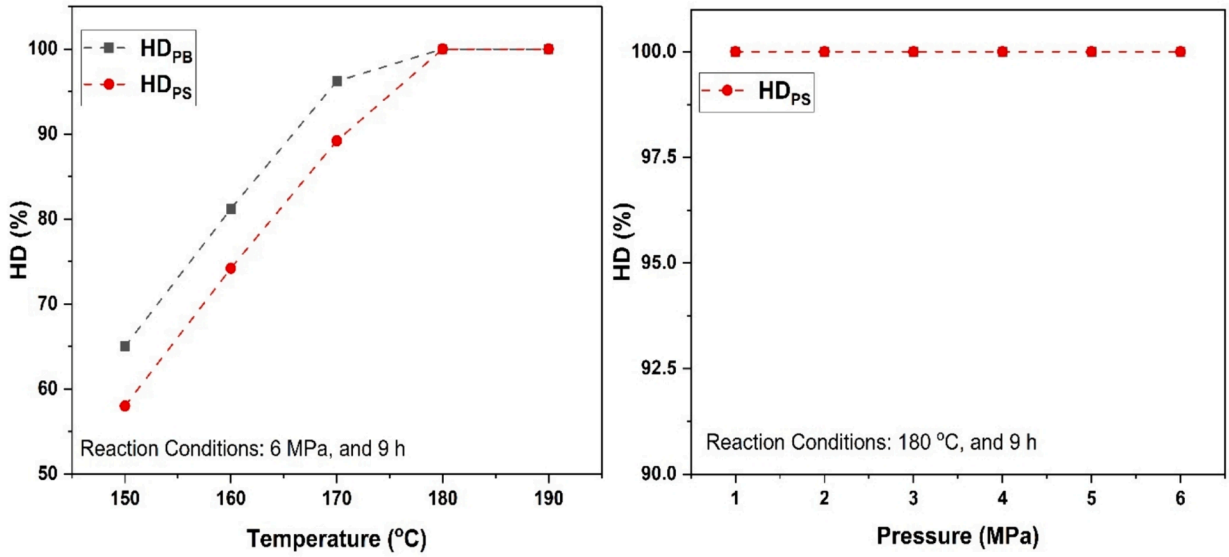

Fig. 12. Pt/MWCNTs catalyst performance on SBS hydrogenation.

Table 1
GPC data of SBS and CBC.

Polymer	*Mw* (g/mol)	*Mn* (g/mol)	Polydispersity (PDI)
SBS	169,927	40,301	4.2
CBC	112,393	24,934	4.5

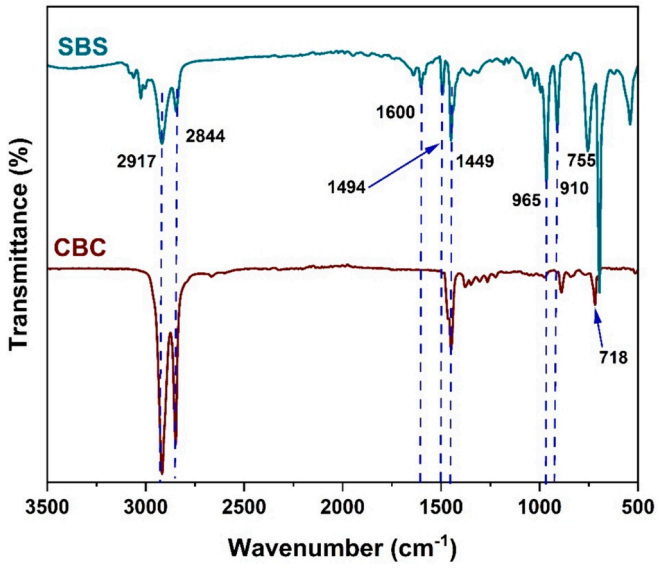

Fig. 13. FTIR of SBS and CBC polymers.

molecules of polymer drastically conformed to wrap around the CNTs. Michael Zaiser (Yang et al., 2005) conducted force-field-based molecular dynamics simulations to investigate the physisorption behavior of polymers on CNTs. The simulation was conducted to model the intermolecular interactions between two polymers and between carbon nanotubes (CNTs) and polymers. During the process of adsorption, the mutual attraction between two polymers gradually declines, causing the segments of polymer chains to separate and form a coating on the CNTs.

M. A. Pasquinelli (Tallury and Pasquinelli, 2010) explored the interaction between CNTs and polymers with different structural

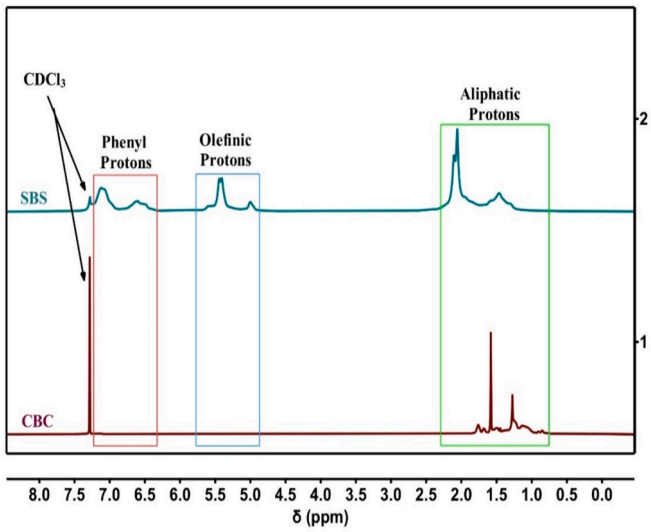

Fig. 14. ^{1}H NMR of SBS and CBC.

arrangements in their main chain and side groups. It was observed that the morphology of the polymer chains adhered to CNTs was affected by the chemical composition and structure of the polymer. Based on their research, the chains are expected to undergo translational movement throughout the length of the CNTs. Thus, we may deduce the physical adsorption characteristics of SBS chains on CNTs under the given solvent conditions from the aforementioned research. Fig. 11 demonstrates that throughout the process, the SBS coils have the potential to undergo structural changes and either wrap around or extend along the surface of CNTs.

The electron-rich structure of CNTs creates an ideal environment for a robust interaction between the polymer chains (containing C-H groups and/or aromatic groups) and the surface of the CNTs during physical adsorption.

3.3. *Effect of reaction parameters*

Pt/MWCNTs have been proven to be an effective catalyst for the selective hydrogenation of polybutadiene and polystyrene blocks in SBS. The effect of reaction parameters (temperature and pressure) was

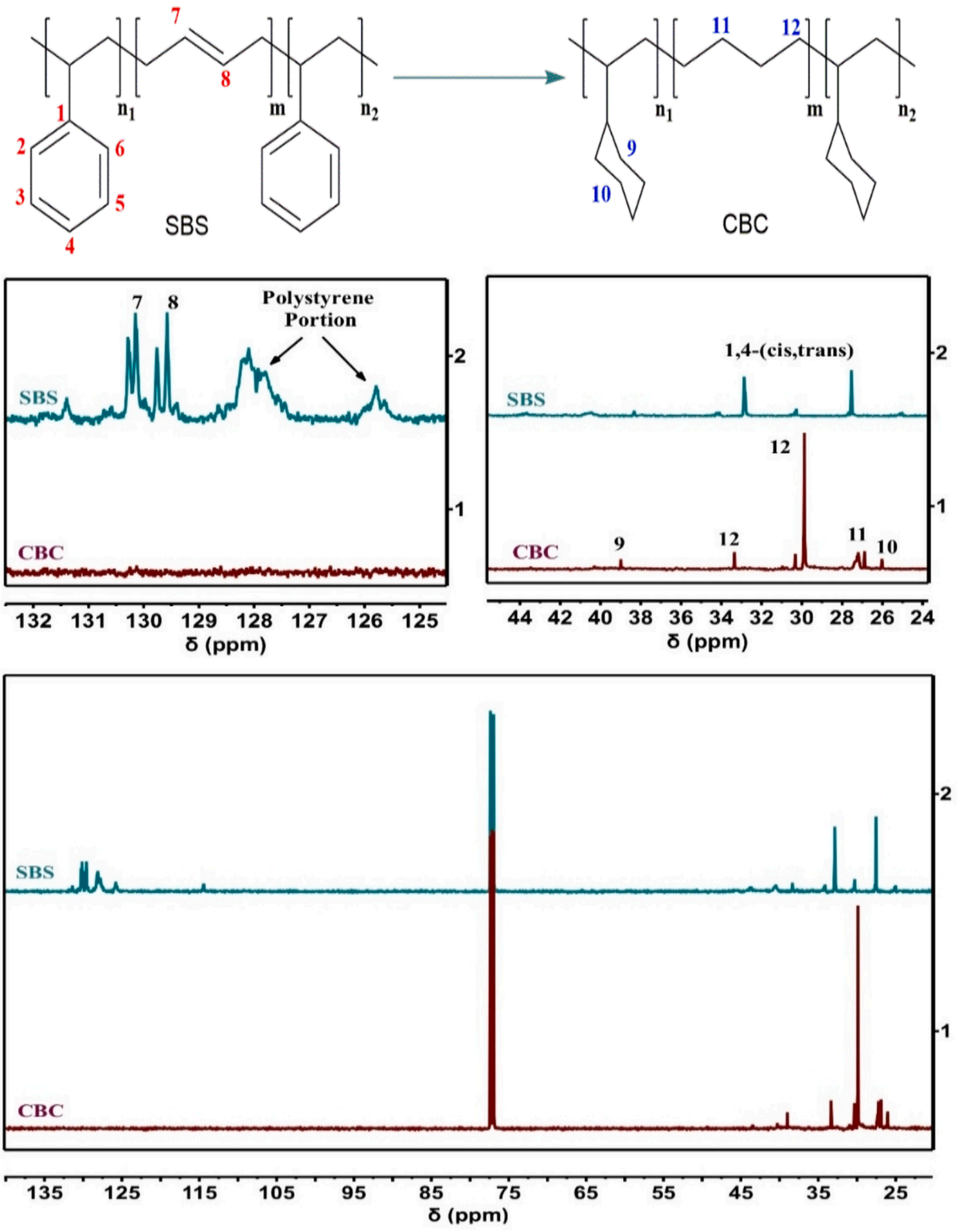

Fig. 15. ^{13}C NMR of SBS and CBC.

investigated. A series of catalytic hydrogenation experiments were performed in an autoclave reactor (Fig. 2) with Pt/MWCNTs as the model catalyst. From the experiments it was noticeable that the hydrogenation of double bonds is faster than the hydrogenation of benzene rings. The reason for this phenomenon is attributed to the larger π-bonds and stability in benzene rings than that in C═C double bonds (De Sarkar et al., 1999; Yan and Cao, 2023). As illustrated in Fig. 12, as the temperature of the reaction raised from 150 °C to 160 °C the hydrogenation degree significantly increased from 58 % (HD_{PS}) and 65 % (HD_{PB}) to 74.2 % (HD_{PS}) and 81.2 % (HD_{PB}). The further increase in reaction temperature to 170 °C has improved the hydrogenation degree up to 89.2 % (HD_{PS}) and 96.2 % (HD_{PB}). The complete hydrogenation (100 %) of benzene rings (HD_{PS}) and C═C double bonds ($HD_{PB)}$ was achieved at 180 °C after 9 h at 6 MPa and 500 rpm. The impact of H_2 pressure on SBS

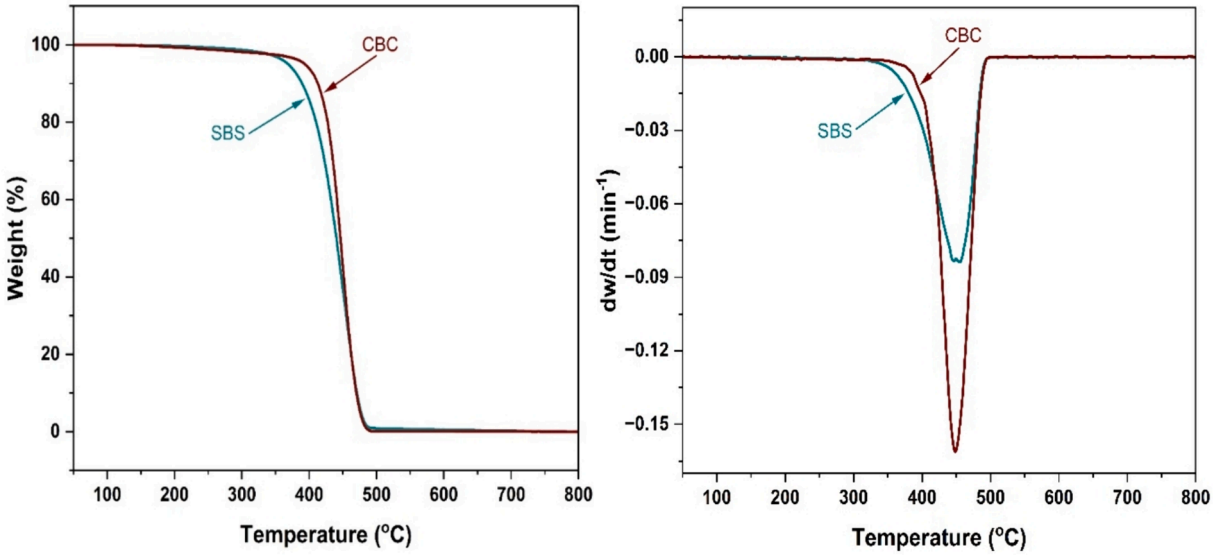

Fig. 16. Thermogravimetric (TG) and thermogravimetric derivative (DTG) curves of SBS and CBC.

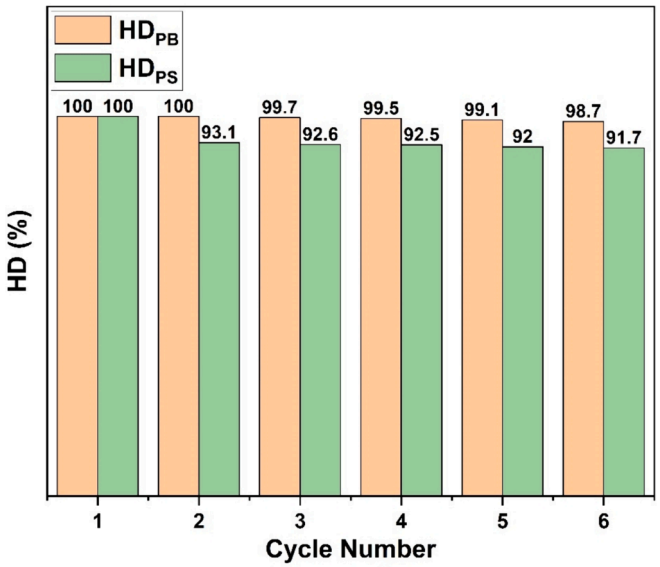

Fig. 17. Recyclability of Pt/MWCNTs catalyst in SBS hydrogenation.

hydrogenation was also examined within the range of 1 to 6 MPa at a temperature of 180 °C. Fig. 12 demonstrates that the SBS hydrogenation remains consistent across different pressures, suggesting that the presence of H_2 does not significantly impact the hydrogenation process or alter the ultimate conversion rate. This may be attributed to the excessive amount of H_2 already present in the system.

3.4. Structure and properties of SBS before and after hydrogenation

The molecular weight (*Mw*), molecular number (*Mn*), and polydispersity of SBS and cyclic block copolymer (CBC) were determined using Gel Permeation Chromatography (GPC). The details are tabulated in Table 1.

The structure of SBS and CBC were analyzed via FTIR, ^{1}H NMR and ^{13}C NMR. Fig. 13 depicts the Fourier Transform Infrared (FTIR) spectra of SBS and CBC. In the spectrum of SBS, prominent peaks are observed at 2844 cm^{-1}, 2917 cm^{-1}, and 3100 cm^{-1}, corresponding to the vibrational stretching of C−H (sp^2-unsaturated) bonds. The peaks observed at 1600 cm^{-1} and 1494 cm^{-1} correspond to distinctive C═C stretching peaks of the aromatic ring. The peaks observed at 755 cm^{-1}, 910 cm^{-1}, and 965 cm^{-1} correspond to the vibrations of 1,4-cis C═C and 1,4-trans C═C, respectively. In the case of CBC, the peak at 718 cm^{-1} is the vibration of C–CH_2 resulting from the saturation of the double bonds. However, all the double bond peaks are not detected and the peaks at 2917 cm^{-1}, and 2844 cm^{-1} as a confirmation of the saturation of sp^2-hybridized C-atom in SBS.

Fig. 14 is the illustration of ^{1}H NMR of SBS and CBC, the $CDCl_3$ solvent has a clear peak at 7.26 ppm. The H-NMR of SBS shows, the 1,2-vinyl peaks at 5.1 ppm, 1,4-trans peaks at 5.5 ppm, 1,4-cis peaks at 5.7 ppm, whereas, on hydrogenation –CH_2– peaks in (−CH_2–CH═CH−CH_2–) at 2.1 ppm, and peaks from 6.5 ppm to 7.4 ppm benzene ring are disappeared, as a results chemical shifts of –CH_2– and –CH– in all repeating units have overlapped in the range of 1.4 ppm–2.4 ppm, which correspond to the conversion of SBS into CBC.

In Fig. 15 (^{13}C NMR spectrum), the C═C chemical shifts (129.4–131.5 ppm), of SBS have disappeared, while chemical shifts (25.9–38.9 ppm), corresponding to the –CH_2– appeared in CBC. Moreover, the chemical shifts of the polystyrene segment (128 ppm and 125.7 ppm) disappeared and simultaneously appeared at 38.9 ppm and 25.9 ppm, corresponding to cyclohexyl. Finally, both FTIR and ^{1}H NMR results supported the findings, indicating that the SBS had fully hydrogenated into CBC.

Thermogravimetric (TG) analysis of SBS and CBC was carried out to investigate their thermal properties. Fig. 16 shows the thermograms of SBS and CBC based on decomposition temperature. SBS shows a decomposition temperature of 407 °C, and CBC shows a decomposition temperature of 423 °C. Based on the comparison between SBS and CBC thermograms, SBS has lower heat resistance than CBC due to the presence of benzene rings and unsaturated double bonds.

3.5. Stability and regeneration of Pt/MWCNTs on SBS hydrogenation

To check the stability and the reusability of Pt/MWCNTs catalyst on SBS hydrogenation, Pt/MWCNTs was used for the recovery experiments at 180 °C, 6 MPa, 500 rpm, and 9 h. The catalyst after each run was filtrated and washed with cyclohexane. As illustrated in Fig. 17 the hydrogenation degree of SBS (HD_{PS} and HD_{PB}) decreased slightly due to the loss of catalyst during the filtration and washing, indicating the excellent stability and reusability of the Pt/MWCNTs catalyst. Overall, the synthesized Pt/MWCNTs catalyst exhibits excellent hydrogenation

activity, stability, and recyclability in the heterogeneous hydrogenation of SBS, which is favorable and significant for their future practical applications.

4. Conclusion

A highly active and selective Pt NPs decorated multi-walled carbon nanotubes (Pt/MWCNTs) catalyst has been successfully synthesized, it showed high activity and selectivity for the catalytic hydrogenation of SBS. The Pt/MWCNTs catalyst possesses well-dispersed Pt nanoparticles, a high specific surface area (159.5501 m^2/g), and a mesoporous structure. The catalytic hydrogenation of SBS via Pt/MWCNTs has achieved a 100 % hydrogenation of polystyrene and polybutadiene blocks in a styrene–butadiene–styrene (SBS) copolymer, implying that the Pt/MWCNTs catalyst is highly effective and can eliminate the diffusion limitation and enhance the accessibility of SBS molecules into the active sites. This research provides highly effective and selective Pt/MWCNTs for macromolecular hydrogenation.

CRediT authorship contribution statement

Alaaddin M.M. Saeed: Writing – original draft, Formal analysis. **Gui-Ping Cao:** Writing – review & editing, Supervision, Project administration, Funding acquisition. **Ahmed S. Al-Fatesh:** Writing – review & editing. **Salwa B. Alreshaidan:** Writing – review & editing. **Nawab Ali:** Writing – review & editing. **Mustapha Sani Shehu:** Writing – review & editing. **Jun-Yang Yan:** Writing – review & editing.

Declaration of competing interest

The authors declare that they have no known competing financial interests or personal relationships that could have appeared to influence the work reported in this paper.

Acknowledgment

We sincerely appreciate the National Natural Science Foundation of China, Shanghai Municipal Commission of Science and Technology, China Scholarship Council, and Collage of International Education of East China University of Science and Technology for their financial support. We would also extend our sincere appreciation to Researchers Supporting Project Number (RSPD2024R779), King Saud University, Riyadh, Saudi Arabia.

References

Avcioglu, G.S., Ficicilar, B., Bayrakceken, A., et al., 2015. High performance PEM fuel cell catalyst layers with hydrophobic channels. Int. J. Hydrogen Energy. 40, 7720–7731. https://doi.org/10.1016/j.ijhydene.2015.02.004.

Bonet, F., Delmas, V., Grugeon, S., et al., 1999. Synthesis of monodisperse Au, Pt, Pd, Ru and Ir nanoparticles in ethylene glycol. Nanostruct. Mater. 11, 1277–1284. https://doi.org/10.1016/S0965-9773(99)00419-5.

Cao, C.-Y., Qian, S.-K., Cao, G.-P., et al., 2024. A new α-CBC polymer with elevated heat-resistance prepared via catalytic hydrogenation of α-methylstyrene-butadiene-styrene terpolymer over NixPd/NCNT@MFN monolithic catalyst. J. Polym. Res. 31, 187. https://doi.org/10.1007/s10965-024-04023-2.

Chen, P., Chew, L.M., Xia, W., 2013. The influence of the residual growth catalyst in functionalized carbon nanotubes on supported Pt nanoparticles applied in selective olefin hydrogenation. J. Catal. 307, 84–93. https://doi.org/10.1016/j.jcat.2013.06.030.

Chen, J., Ma, L., Cheng, T., et al., 2018. Stable and recyclable Pd catalyst supported on modified silica hollow microspheres with macroporous shells for enhanced catalytic hydrogenation of NBR. J. Mater. Sci. 53, 15064–15080. https://doi.org/10.1007/s10853-018-2698-1.

Chuang, L., Shao, Z., Pang, M., et al., 2012. Carbon nanotubes supported mono- and bimetallic Pt and Ru catalysts for selective hydrogenation of phenylacetylene. Ind. Eng. Chem. Res. 51, 4934–4941. https://doi.org/10.1021/ie202342a.

De Sarkar, M., De, P.P., Bhowmick, A.K., 1999. Influence of hydrogenation and styrene content on the unaged and aged properties of styrene-butadiene copolymer. J. Mater. Sci. 34, 1741–1747. https://doi.org/10.1023/A:1004542705317.

Gonçalves, L.P.L., Meledina, M., Meledin, A., et al., 2022. Understanding the importance of N−doping for CNT-supported Ni catalysts for CO2 methanation. Carbon 195, 35–43. https://doi.org/10.1016/j.carbon.2022.03.059.

Gu, Y., Norton, J.R., Salahi, F., et al., 2021. Highly selective hydrogenation of C═C bonds catalyzed by a rhodium hydride. J. Am. Chem. Soc. 143, 9657–9663. https://doi.org/10.1021/jacs.1c04683.

Guo, Z., Chen, Y., Li, L., et al., 2010. Carbon nanotube-supported Pt-based bimetallic catalysts prepared by a microwave-assisted polyol reduction method and their catalytic applications in the selective hydrogenation. J. Catal. 276, 314–326. https://doi.org/10.1016/j.jcat.2010.09.021.

Han, K.-Y., Zuo, H.-R., Zhu, Z.-W., et al., 2013. High performance of palladium nanoparticles supported on carbon nanotubes for the hydrogenation of commercial polystyrene. Ind. Eng. Chem. Res. 52, 17750–17759. https://doi.org/10.1021/ie401184h.

Hemraj-Benny, T., Tobar, N., Carrero, N., et al., 2018. Microwave-assisted synthesis of single-walled carbon nanotube-supported ruthenium nanoparticles for the catalytic degradation of Congo red dye. Mater. Chem. Phys. 216, 72–81. https://doi.org/10.1016/j.matchemphys.2018.05.081.

Jin, X., Yan, J., Liu, X., et al., 2024. Spatial confinement of Pt nanoparticles in carbon nanotubes for efficient and selective H2 evolution from methanol. Adv. Sci. 11, 2306893. https://doi.org/10.1002/advs.202306893.

Kardimi, K., Tsoufis, T., Tomou, A., et al., 2012. Synthesis and characterization of carbon nanotubes decorated with Pt and PtRu nanoparticles and assessment of their electrocatalytic performance. Int. J. Hydrogen Energy 37, 1243–1253. https://doi.org/10.1016/j.ijhydene.2011.09.143.

Khar'kova, E.M., Rozantseva, L.E., Frolov, V.M., 2011. Hydrogenation of unsaturated polymers under the action of oligoallene complexes of transition metals. Polym. Sci. Ser. B 53, 420. https://doi.org/10.1134/S1560090411070049.

Krishnapriya, R., Nizamudeen, C., Mourad, A.H.I., 2023. Platinum nanoparticles decorated multiwalled carbon nanotube composites as highly transparent, bifacial counter electrodes for dye-sensitized solar cells. Mater. Renew. Sustain. Energy 12, 257–265. https://doi.org/10.1007/s40243-023-00247-2.

Li, C., Xu, S., Yue, Y., et al., 2016. Thermal characterization of carbon nanotube fiber by time-domain differential Raman. Carbon 103, 101–108. https://doi.org/10.1016/j.carbon.2016.03.003.

Luo, Z.-H., Feng, M., Lu, H., et al., 2019. Nitrile butadiene rubber hydrogenation over a monolithic Pd/CNTs@Nickel foam catalysts: tunable CNTs morphology effect on catalytic performance. Indus. Eng. Chem. Res. 58, 1812–1822. https://doi.org/10.1021/acs.iecr.8b04688.

Ma, S.-Y., Li, H.-H., Hu, B.-C., et al., 2017. Synthesis of low Pt-based quaternary PtPdRuTe nanotubes with optimized incorporation of Pd for enhanced electrocatalytic activity. J. Am. Chem. Soc. 139, 5890–5895. https://doi.org/10.1021/jacs.7b01482.

McCarthy, B., Coleman, J.N., Czerw, R., et al., 2002. A microscopic and spectroscopic study of interactions between carbon nanotubes and a conjugated polymer. J. Phys. Chem. B 106, 2210–2216. https://doi.org/10.1021/jp013745f.

Miceli, M., Frontera, P., Macario, A., et al., 2021. Recovery/reuse of heterogeneous supported spent catalysts. Journal 11. https://doi.org/10.3390/catal11050591.

Milone, C., Shahul Hameed, A.R., Piperopoulos, E., Santangelo, S., Lanza, M., Galvagno, S., 2011. Catalytic wet air oxidation of p-coumaric acid over carbon nanotubes and activated carbon. Ind. Eng. Chem. Res. 50, 9043–9053. https://doi.org/10.1021/ie200492g.

Pang, M., Li, C., Ding, L., et al., 2010. Microwave-assisted preparation of Mo2C/CNTs nanocomposites as efficient electrocatalyst supports for oxygen reduction reaction. Ind. Eng. Chem. Res. 49, 4169–4174. https://doi.org/10.1021/ie901741c.

Pei, A., Li, G., Zhu, L., et al., 2022. Nickel hydroxide-supported Ru single atoms and Pd nanoclusters for enhanced electrocatalytic hydrogen evolution and ethanol oxidation. Adv. Funct. Mater. 32, 2208587. https://doi.org/10.1002/adfm.202208587.

Pei, A., Xie, R., Zhang, Y., et al., 2023. Effective electronic tuning of Pt single atoms via heterogeneous atomic coordination of (Co, Ni)(OH)2 for efficient hydrogen evolution. Energy Environ. Sci. 16, 1035–1048. https://doi.org/10.1039/D2EE02785B.

Tallury, S.S., Pasquinelli, M.A., 2010. Molecular dynamics simulations of flexible polymer chains wrapping single-walled carbon nanotubes. J. Phys. Chem. B 114, 4122–4129. https://doi.org/10.1021/jp908001d.

Tong, H., Li, H.-L., Zhang, X.-G., 2007. Ultrasonic synthesis of highly dispersed Pt nanoparticles supported on MWCNTs and their electrocatalytic activity towards methanol oxidation. Carbon 45, 2424–2432. https://doi.org/10.1016/j.carbon.2007.06.028.

Wang, S., Ge, B., Yang, Z., et al., 2024. Construction of highly active Pd–Ti3+ sites in defective Pd/TiO2 catalysts for efficient hydrogenation of styrene–butadiene–styrene. ACS Catal. 14, 1432–1442. https://doi.org/10.1021/acscatal.3c04811.

Wei, Q., Chen, X., He, Y., et al., 2022. Ni Nanoparticles supported on N-doped carbon nanotubes for efficient hydrogenation of C5 hydrocarbon resins under mild conditions. Micropor. Mesopor. Mater. 333, 111727. https://doi.org/10.1016/j.micromeso.2022.111727.

Yan, J.-Y., Cao, G.-P., 2023. Advances in the catalytic hydrogenation and properties of unsaturated polymers. Macromolecules 56, 3774–3808. https://doi.org/10.1021/acs.macromol.2c02333.

Yan, J.-Y., Cao, G.-P., Cao, C.-Y., et al., 2024. Mechanism and kinetics of polystyrene hydrogenation catalyzed by a monolithic Pd-NCNTs@FN catalyst. Ind. Eng. Chem. Res. 63, 6906–6921. https://doi.org/10.1021/acs.iecr.3c04622.

Yang, M., Koutsos, V., Zaiser, M., 2005. Interactions between polymers and carbon nanotubes: a molecular dynamics study. J. Phys. Chem. B 109, 10009–10014. https://doi.org/10.1021/jp0442403.

Yang, L., Pan, Q., Rempel, G.L., 2012. Recovery of Wilkinson's catalyst from polymer based matrix using carbon dioxide expanded methanol. J. Supercrit. Fluids 68, 104–112. https://doi.org/10.1016/j.supflu.2012.04.016.

Yang, L., Pan, Q., Rempel, G.L., 2013. Development of a green separation technique for recovery of Wilkinson's catalysts from bulk hydrogenated nitrile butadiene rubber. Catal. Today 207, 153–161. https://doi.org/10.1016/j.cattod.2012.02.024.

Yao, Y., Izumi, R., Tsuda, T., et al., 2019. Platinum and PtNi nanoparticle-supported multiwalled carbon nanotube electrocatalysts prepared by one-pot pyrolytic synthesis with an ionic liquid. ACS Appl. Energy Mater. 2, 4865–4872. https://doi.org/10.1021/acsaem.9b00561.

Zhang, S., A. Pei, G. Li, et al., 2022. Pd/CuO–Ni(OH)2/C as a highly efficient and stable catalyst for the electrocatalytic oxidation of ethanol††Electronic supplementary information (ESI) available. Green Chem. 24, 2438–2450. doi:10.1039/d1gc04799j.

Zhang, J., Hu, W., Qian, B., et al., 2023. Tuning hydrogenation chemistry of Pd-based heterogeneous catalysts by introducing homogeneous-like ligands. Nat. Commun. 14, 3944. https://doi.org/10.1038/s41467-023-39478-2.

Zhu, L., Sun, Y., Zhu, H., et al., 2022a. Effective ensemble of Pt single atoms and clusters over the (Ni, Co)(OH)2 substrate catalyzes highly selective, efficient, and stable hydrogenation reactions. ACS Catal. 12, 8104–8115. https://doi.org/10.1021/acscatal.2c01901.

Zhu, L., Zhang, H., Zhu, H., et al., 2022b. Controlling nanostructures of PtNiCo/C trimetallic nanocatalysts and relationship of structure-catalytic performance for selective hydrogenation of nitroarenes. J. Catal. 413, 978–991. https://doi.org/10.1016/j.jcat.2022.08.012.

Zhuchkov, D.P., Nenasheva, M.V., Terenina, M.V., et al., 2021. Polymeric heterogeneous catalysts in the hydroformylation of unsaturated compounds. Pet. Chem. 61, 1–14. https://doi.org/10.1134/S0965544121010011.

Zou, C., Tan, C., Chen, C., 2023. Heterogenization strategies for nickel catalyzed synthesis of polyolefins and composites. Acc. Mater. Res. 4, 496–506. https://doi.org/10.1021/accountsmr.2c00263.